BUTTERWORTH HEINEMANN

Induced flow in isothermally heated vertical annuli with two rotating boundaries

Z. Kodah
Mechanical Engineering Department, Jordan University of Science and Technology, Irbid, Jordan

M. A. I. El-Shaarawi
King Fahd University of Petroleum and Minerals, Dhahran, Saudi Arabia

This paper is about induced laminar flow through an open-ended vertical annulus with two rotating boundaries, one of which is isothermally heated, while the other is perfectly insulated. The boundary-layer equations governing this case have been numerically solved, and results are presented for a fluid of Pr = 0.7 in an annulus of radius ratio 0.9. These results clarify the characteristics of the induced flow caused by isothermally heating one of the two rotating boundaries. Moreover, the results presented show the effect of outer cylinder rotation on the adiabatic wall temperature, the heat absorbed by the fluid, and the relationship between the annulus height and the induced flow rate.

Keywords: Induced flow characteristics; rotational parameter; angular velocities; annulus radius ratio

Introduction

Coney and El-Shaarawi (1974a, 1974b) investigated the hydrodynamically developing laminar force flow with constant physical properties in the entrance region of concentric annuli with rotating inner walls. They showed that, provided the inner cylinder rotational speed is insufficient to generate hydrodynamic instability (Astill 1964) and/or Taylor vortices (Taylor 1923), the inner cylinder rotation slightly affects the heat transfer in the laminar regime.

El-Shaarawi and Sarhan (1981) presented numerical results for natural convection flow of a fluid of Pr = 0.7 in an open-ended, vertical, concentric annulus of radius ratio 0.5 with a rotating inner wall under the thermal boundary conditions of one wall being isothermal and the opposite wall adiabatic. El-Shaarawi and Khamis (1987) presented numerical results for laminar natural convection through an open-ended, vertical annulus with a rotating inner cylinder, one uniformly heated boundary, and one adiabatic boundary. Results of both investigations (El-Shaarawi and Sarhan; El-Shaarawi and Khamis) show that heating the inner cylinder always has stabilizing effects; whereas, heating the outer cylinder has either destabilizing or stabilizing effects.

Soundalgekar and Sarma (1986) numerically investigated the developing laminar forced flow in an annulus between two co-rotating cylinders. El-Shaarawi and Kodah (1990) studied the developing natural convection in an open-ended, vertical annulus with two co-rotating or counter-rotating boundaries, a uniformly heated inner wall, and an adiabatic outer wall. To the best of the authors' knowledge, no investigations are available in the literature concerning induced flow in vertical, concentric annuli with two rotating boundaries under the isothermal boundary condition. The lack of either experimental or theoretical data on this subject motivated the present work. This work presents the induced flow characteristics in an annulus whose two boundaries are rotating in either the same or opposite directions, and one of these boundaries is isothermally heated, while the other is perfectly insulated. Two thermal boundary conditions are considered; namely, case (I) in which the inner cylinder is isothermally heated, while the outer cylinder is perfectly insulated; and case (0) in which the outer cylinder is the isothermally heated boundary, while the inner cylinder is adiabatic.

Governing equations and method of solution

Consider a vertical, open-ended concentric annulus whose inner and outer cylinders rotate with constant angular velocities Ω_1 and Ω_2, respectively, and either its inner or its outer wall is isothermally heated; whereas, the other wall is perfectly insulated. The heat added to (or removed from) one of the annulus walls engenders an upward (or downward) natural flow in the annular gap between the two cylindrical walls. This induced flow is assumed to be steady and axisymmetric, with no internal heat generation, negligible viscous dissipation, and the fluid enters the bottom (in the case of heating) or the top (in the case of cooling) of the annulus with a flat velocity profile at a value equal to the mean axial velocity in the annular gap u_o, and with a uniform temperature profile at a value equal to the ambient temperature t_o. The physical properties of the fluid are assumed to be independent of location and temperature, but the density is allowed to vary with temperature in only the body force term of the vertical (axial momentum) equation. Furthermore, the hydrodynamic and thermal boundary-layer simplifications are assumed to be

Address reprint requests to Dr. Kodah at the Mechanical Engineering Department, Jordan University of Science and Technology, P.O. Box 3030, Irbid, Jordan.

Received 2 April 1991; accepted 12 August 1994

Int. J. Heat and Fluid Flow 16: 36–42, 1995

655 Avenue of the Americas, New York, NY 10010

0142-727X/95/$10.00
SSDI 0142-727X(94)00003-U

Notation

a local heat transfer coefficient based on area of heat transfer surface
$q/(t_w - t_o) = \mp k \left.\frac{\partial t}{\partial r}\right|_w \Big/ (t_m - t_w)$;
the minus and plus signs are, respectively, for heating (upward flow) and cooling (downward flow) at the inner boundary [case (I)] and vice versa at the outer boundary [case (0)]

$\bar{a}$ average heat transfer coefficient over the annulus height based on area of heated wall,
$\int_0^l a \, dz/l = \pm \bar{h}/\pi D_w (t_w - t_0) l$,
the plus and minus signs are for upward (heating) and downward (cooling) flows, respectively

b annular gap width, $(r_2 - r_1)$

c_p specific heat of fluid at constant pressure

D equivalent (hydraulic) diameter of annulus, $2b$

D_w diameter of heated wall

$\int_{r_1}^{r_2} 2\pi r u \, dr = \pi(r_2^2 - r_1^2) u_0$

F dimensionless volumetric flow rate,
$f/\pi l \mathrm{Gr}^* \nu = 2 \int_N^1 RU \, dR = (1 - N^2) U_0$

F_{fd} fully developed value of F

g gravitational body force per unit mass

Gr Grashof number, $\pm g\beta(t_w - t_o)D^3/\nu^2$; the plus and minus signs and for heating (upward flow) and cooling (downward flow), respectively

Gr^* modified Grashof number, $\mathrm{Gr} \cdot D/l$

h heat absorbed or lost by fluid from entrance up to a particular elevation in the annulus, $\pm \rho_o f c_p (t_m - t_o)$; the plus and minus signs are for heating and cooling, respectively

$\bar{h}$ heat absorbed or lost by fluid from entrance up to the annulus exit; i.e., value of h at $z = l$, $\pm \rho_o c_p f(\bar{t}_m - t_o)$; the plus and minus signs are for heating and cooling, respectively

H dimensionless heat absorbed or lost from entrance up to a particular elevation,
$\pm h/\pi \rho_o c_p \nu \, \mathrm{Gr}^* l (t_w - t_o) = 2 \int_N^1 UTR = FT_m$
plus and minus signs are respectively for heating and cooling

$\bar{H}$ dimensionless heat absorbed or lost from entrance up to annulus exit; i.e., value of H at $z = l$, $\pm h/\pi \rho_o c_p \nu \, \mathrm{Gr}^* l (t_w - t_o)$

H_{fd} fully developed value of H

k thermal conductivity of fluid

l height of annulus

L dimensionless annulus height, $1/\mathrm{Gr}^*$

N annulus radius ratio, r_1/r_2

Nu local Nusselt number,
$aD/k = 2(1 - N) \left.\frac{\partial T}{\partial R}\right|_w \Big/ (1 - T_m)$

$\overline{\mathrm{Nu}}$ average Nusselt number, $\bar{a}D/k = \bar{H} \, \mathrm{Ra}^* \, D/D_w$

p pressure of fluid at any point inside the channel

p' pressure defect at any point, $(p - p_s)$

p_o pressure of fluid at annulus entrance

p_s hydrostatic pressure at any particular elevation, $\pm \rho_o g z$; the minus and plus signs are for upward (heating) and downward (cooling) flows, respectively

p_{wo} pressure of fluid at outer boundary

P dimensionless pressure defect, $p' r_2^4/\rho_o l^2 \nu^2 (\mathrm{Gr}^*)^2$

P_{wo} dimensionless pressure defect at outer boundary

Pr Prandtl number, $\mu c_p/k$

q heat flux at heat transfer boundary, which is positive in the case of heating and negative in the case of cooling, $\pm k(\partial t/\partial r)_w$; the minus and plus signs are respectively for cases (I) and (0) when there is heating, and vice versa when there is cooling

r radial coordinate

r_1 inner radius of annulus

r_2 outer radius of annulus

R dimensionless radial coordinate, r/r_2

Ra Rayleigh number, $\mathrm{Gr} \cdot \mathrm{Pr}$

Ra* modified Rayleigh number, $\mathrm{Gr}^* \cdot \mathrm{Pr}$

Re axial Reynolds number $u_o D/\nu$

t fluid temperature at any point

t_{ad} adiabatic wall temperature

t_m mixing cup temperature over any cross section
$\int_{r_1}^{r_2} utr \, dr \Big/ \int_{r_1}^{r_2} ur \, dr$

$\bar{t}_m$ mixing cup temperature over the exit cross section; i.e., value of t_m at $z = l$

t_o fluid temperature at annulus entrance

T dimensionless temperature at any point, $(t - t_o)/(t_w - t_o)$

T_{ad} dimensionless adiabatic wall temperature, $(t_{ad} - t_o)/(t_w - t_o)$

T_m dimensionless mixing cup temperature over any cross section
$(t_m - t_o)/(t_w - t_o) = \int_N^1 UTR \, dR \Big/ \int_N^1 UR \, dR$

$\bar{T}_m$ mixing cup temperature at exit cross section; i.e., value of T_m at $z = l$

Ta Taylor number, $2\Omega_1^2 r_1^2 b^3/\nu^2(r_1 + r_2)$

Ta* modified Taylor number, $\mathrm{Ta}\,(b/1)^2$

u axial velocity component at any point

u_o entrance axial velocity,
$\int_{r_1}^{r_2} 2ur \, dr/(r_2^2 - r_1^2)$

u_{fd} fully developed axial velocity component

U dimensionless axial velocity component, $ur_2^2/\nu l \, Gr^*$

U_o dimensionless axial velocity at annulus entrance, $u_o r_2^2/\nu l \, Gr^*$

U_{fd} dimensionless fully developed axial velocity component

v radial velocity component at any point

v_{fd} fully developed radial velocity component (equals zero)

V dimensionless radial velocity component, vr_2/ν

w tangential velocity component, at any point

w_{fd} fully developed tangential velocity component

W dimensionless tangential velocity component, $w/\Omega_1 r_1$

W_{fd} dimensionless fully developed tangential velocity component, $w_{fd}/\Omega_1 r_1$

z axial coordinate

Z dimensionless axial coordinate, $z/l \, Gr^*$

Greek symbols

α thermal diffusivity of fluid, $k/\rho_o c_p$

β volumetric coefficients of thermal expansion

δ_u axial-velocity–boundary-layer thickness

δ_w tangential–velocity-boundary layer thickness

δ_θ tangential boundary-layer displacement thickness
$\int_{r_1}^{r_2} w \, dr/r_1 \Omega$

δ_θ^* dimensionless tangential boundary-layer displacement thickness, $\delta_{\theta/b}$

μ dynamic fluid viscosity

ν kinematic fluid viscosity, μ/ρ_o

ρ fluid density at temperature t, $\rho_o[1 - \beta(t - t_o)]$

ρ_o fluid density at inlet fluid temperature

ϕ dimensionless radial coordinate, $(r - r_1)/(r_2 - r_1)$

Ω ratio between angular velocities of the cylinders, Ω_2/Ω_1

Ω_1 angular velocity of inner cylinder

Ω_2 angular velocity of outer cylinder

applicable; i.e., axial diffusions of momentum and heat are negligible, as compared with their transverse (radial) counterparts, and the radial velocity component is negligible, as compared with the axial and tangential counterparts.

Under the above assumptions, the equations that govern the induced fluid motion and heat transfer, in their dimensionless forms, using the nondimensional parameters given in the notation, are as follows:

$$\frac{\partial V}{\partial R}+\frac{V}{R}+\frac{\partial U}{\partial Z}=0 \tag{1}$$

$$\frac{W^2}{R}=\frac{(1-N)^3(1+N)}{2F^2}\frac{\mathrm{Re}^2}{\mathrm{Ta}}\frac{\partial P}{\partial R} \tag{2}$$

$$V\frac{\partial W}{\partial R}+U\frac{\partial W}{\partial z}=\frac{\partial^2 W}{\partial R^2}+\frac{1}{R}\frac{\partial W}{\partial R}-\frac{W}{R^2} \tag{3}$$

$$V\frac{\partial U}{\partial R}+U\frac{\partial U}{\partial Z}=-\frac{\partial P}{\partial Z}+\frac{T}{16(1-N)^4}+\frac{\partial^2 U}{\partial R^2}+\frac{1}{R}\frac{\partial U}{\partial R} \tag{4}$$

$$V\frac{\partial T}{\partial R}+U\frac{\partial T}{\partial Z}=\frac{1}{\mathrm{Pr}}\left(\frac{\partial^2 T}{\partial R^2}+\frac{1}{R}\frac{\partial T}{\partial R}\right) \tag{5}$$

These five coupled Equations 1–5 are subject to the following boundary conditions:

for

$Z = 0$ and $N < R < 1$, $V = W = T = 0$, $U = U_0$,

and

$P = P_0 = -U_0^2/2$

for

$Z \geq 0$ and $R = N$, $U = V = 0$, $W = 1$,

and

$T = 1$ for case I or $\dfrac{\partial T}{\partial R} = 0$ for case 0

for

$Z \geq 0$ and $R = 1$, $U = V = 0$, $W = \Omega/N$,

and

$\dfrac{\partial T}{\partial R} = 0$ for case I

or

$T = 1$ for case (0)

for

$Z = L$ and $R = 1$, $P = 0$ (6)

In practice, the annulus height is normally known, and it must be known to find the corresponding induced flow rate. However, in the present method, the reversed problem is handled (El-Shaarawi and Sarhan 1981); i.e., we find an unknown channel height for the given flow rate F, Ω, and $\mathrm{Re}^2/\mathrm{Ta}$. Taking into consideration that $\mathrm{Gr} = (1 + N)\mathrm{Re}/\{4(1 - N)F\}$; i.e., $\mathrm{Re}^2/\mathrm{Ta} = 16F^2(\mathrm{Gr}^2/\mathrm{Ta})(1 - N)^2/(1 + N)^2$, the above set of coupled equations are exactly identical to those dimensionless equations that govern the case with a stationary outer boundary (El-Shaarawi and Sarhan), and hence, the finite-difference scheme presented by El-Shaarawi and Sarhan could be used. However, the following five similarity parameters govern the present case: the annulus radius ratio N; the dimensionless volumetric flow rate F; or the dimensionless axial velocity component at annulus entrance U_o, instead of F because $F = (1 - N^2)U_o$); the rotational parameter $\mathrm{Re}^2/\mathrm{Ta}$ that appears in the radial momentum Equation (2) (or $\mathrm{Gr}^2/\mathrm{Ta}$ instead of $\mathrm{Re}^2/\mathrm{Ta}$; and the ratio between angular velocities of cylinders Ω and the Prandtl number (Pr). Values of these five controlling similarity parameters should, therefore, be chosen for each computer run. Then, the computation starts at the entrance of the annulus and continues in the axial direction until the dimensionless pressure defect P at the outer wall of the annulus ceases to be negative (that is, where the maximum pressure at a point in the annular gap becomes equal to the hydrostatic pressure at its elevation). The dimensionless axial distance Z from the entrance of the annulus to the cross section at which $P = 0$ at $R = 1$ establishes the unknown dimensionless height L, and hence, the unknown modified Grashof number Gr* corresponding to the chosen values of the similarity parameters.

Fully developed profiles

There are two velocity boundary layers developing on each of the annulus walls. The axial-velocity–boundary-layer thickness δ_u is inversely proportional to the square root of Reynolds number ($\delta_u \sim 1/\sqrt{\mathrm{Re}}$) (Schlichting 1979), and similarly, the tangential-velocity–boundary-layer thickness δ_w is inversely proportional to the Taylor number raised to the power 1/4 ($\delta_w \sim \mathrm{Ta} - 1/4$). The relative magnitudes of the lengths required for the tangential velocity component and the axial velocity component development is proportional to the ratio δ_w/δ_u, which is proportional to $(\mathrm{Re}^2/\mathrm{Ta})^{1/4}$.

If the annulus is sufficiently high, fully developed conditions may be achieved before the fluid reaches the exit cross section. For free-convection flows in vertical ducts, the single assumption of a fully developed velocity field necessarily means that the flow is also thermally fully developed l(Schlichting 1979). In other words, the thermal development length, for natural convection flows in vertical channels, is shorter, or at most, equal to that of the hydrodynamic development length, irrespective of the value of Prandtl number (Aung 1972). This is, of course, different from the case of pure forced convection, in which the relative magnitudes of the thermal and hydrodynamic development lengths are strongly dependent on the value of Prandtl number.

In the present case, because one of the annulus boundaries is kept isothermal, fully developed conditions are $T = 1$, $\partial/\partial Z = 0$, and $V = 0$. Thus, for fully developed flow, Equations 3 and 4 reduce to the following:

$$\frac{\partial}{\partial R}\left[\frac{1}{R}\frac{\partial}{\partial R}(RW_{\mathrm{fd}})\right]=0 \tag{7}$$

and

$$\frac{1}{R}\frac{\partial}{\partial R}\left(R\frac{\partial U_{\mathrm{fd}}}{\partial R}\right)+\frac{1}{16(1-N)^4}=0 \tag{8}$$

Integrating each of Equations 7 and 8 twice and applying the boundary conditions gives the following fully developed Couette (tangential) and axial velocity profiles, respectively:

$$W_{\mathrm{fd}} = N/1 - N^2[(1 - \Omega)/R - R(1 - \Omega/N^2)] \tag{9}$$

and

$$U_{\mathrm{fd}} = [1 - R^2 - (1 - N^2)(\ln R/\ln N)/64(1 - N)^4 \tag{10}$$

These fully developed velocity profiles provide an analytical check on the numerical solutions to be obtained in sufficiently high annuli. Also, it should be noted that in the present case with an isothermal boundary condition, there is an upper limiting value of the dimensionless volumetric flow rate F.

Using Equation 10 and taking into consideration that $T = 1$ for fully developed flow, the upper-limiting values of the dimensionless volumetric flow rate and heat absorbed (F and H) are as follows

$$F_{fd} = H_{fd} = 2\int_N^1 RU_{fd}\,dR = \frac{1-N^2}{128(1-N)^4}\left[1+N^2+\frac{1-N^2}{\ln N}\right] \quad (11)$$

Results and discussion

For a fluid of Pr = 0.7 in an annulus of $N = 0.9$, more than 120 computer runs were made for each of case (I) and case (0). These computer runs cover some selected ranges of the controlling parameters F, Re^2/Ta, and Ω. Twelve values of $F < F_{fd}$ (0.001, 0.005, 0.01, 0.02, 0.03, ..., 0.09, and 0.095), two values of Re^2/Ta (10 and 1), and more than seven values of Ω (0.00, $\pm$0.45, $\pm$0.90, $\pm$1.8, ...) were chosen.

For the special case of a rotating inner cylinder and a stationary outer cylinder, the development of the tangential boundary-layer displacement thickness (δ_θ) is of special importance. Astill (1964) developed an empirical stability criterion for the onset of hydrodynamic instability in tangentially developing flows. To the authors' knowledge, this is the unique criterion available to date for the location of the axial position of the point of origin of instability in tangentially developing flows. Astill's empirical stability criterion is, in fact, a Taylor number based on the tangential boundary-layer displacement thickness, rather than the gap width. To the authors' knowledge, the only results available in the literature for the development of δ_θ in the free convection regime under the isothermal boundary condition are those of El-Shaarawi and Sarhan (1981), for an annulus of radius ratio 0.5. For this reason, and in order to cover the lack of information in the literature and to facilitate the use of Astill's stability criterion, the developing dimensionless tangential boundary-layer displacement thickness (δ_θ^*) is presented for an annulus of radius ratio 0.9, under the isothermal boundary conditions of cases (I) and (0) in Figs. 1a and 1b, respectively. In each of these two figures, δ_θ^* is presented against the dimensionless axial distance Z (measured from the annulus entrance) for some selected values of the dimensionless flow rate F as a parameter. Each curve (corresponding to a given F) in these two figures ends at $Z = L$. For relatively large values of F, δ_θ^* approaches the fully developed value of 0.490761; again, this provides a check on the adequacy of the present numerical solutions.

Comparing the values δ_θ^* in these two figures, it can be seen that the value of δ_θ^* for case (I) is lower, at the same values of Z and F, than its corresponding value for case (0). Combining this result with Astill's (1964) stability criterion for tangentially developing flows means that thermal boundary conditions (I) engenders a flow that has a more stable tendency than that engendered because of thermal boundary conditions (0). This result is as might be expected because under thermal boundary conditions (I) and (0), negative and positive radial temperature gradients exist, respectively. Becker and Kaye (1962) and Walowit, et al. (1964) have shown that positive and negative radial temperature gradients are destabilizing and stabilizing, respectively.

On the other hand, from either of these two figures, it can be seen that, at the same value of Z, decreasing the value of F causes an increase in the value of δ_θ^*; i.e., according to Astill's (1964) stability criterion, shows more tendency for destabilization. This can be attributed to the fact that F is directly

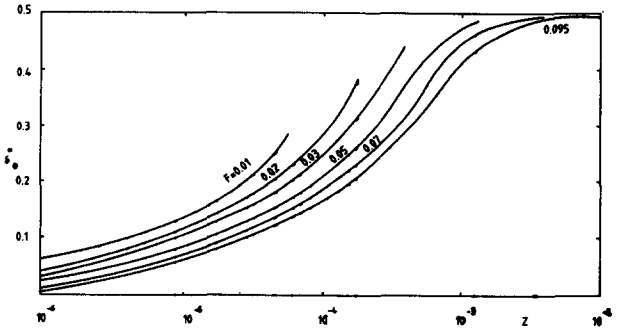

Figure 1(a) Dimensionless tangential boundary-layer displacement thickness against dimensionless axial distance: $N = 0.9$; Pr = 0.7; $Re^2/Ta = 10$; $\Omega = 0$, case (I)

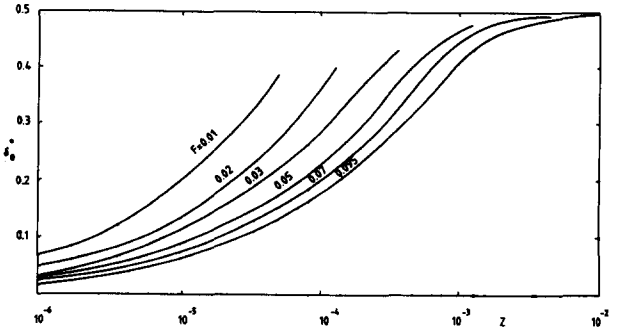

Figure 1(b) Dimensionless tangential boundary-layer displacement thickness against dimensionless axial distance: $N = 0.9$; Pr = 0.7; $Re^2/Ta = 10$; $\Omega = 0$, case (0)

proportional to the axial velocity, and it is known (Chung and Astill 1977) that the presence of a superimposed, low axial flow has a stabilizing effect on the onset of Taylor vortices.

At this stage, it may be instructive to mention that the present results for δ_θ^*, and hence, stability conclusions based on the rates of growth of δ_θ^*, do not consider the effect of kinematic viscosity variation (caused by temperature differences). Simmers and Coney (1980) indicate that the critical Taylor number is higher in diabatic flows than for adiabatic flows because of the dependence of Taylor number on kinematic viscosity. However, Wan and Coney (1982) note that the viscosity variation in air, being small, would not have a strong effect. Their forced flow experiments with a heated outer wall in a vertical annulus suggest a stabilizing effect, rather than the present conclusion based on Astill's (1964) stability criterion, and which is in agreement with conclusions of Becker and Kaye (1962) and Walowit et al. (1964). To the author's knowledge, experimental results are not yet available for the problem of hydrodynamic stability in the free-convection regime. Therefore, experimental programs are needed in this context.

Tables 1 and 2 give, for cases (I) and (0) respectively, the dimensionless annulus height corresponding to each chosen value of F for all the investigated values of Ω and Re^2/Ta. These two tables are of practical importance to designers and engineers. An important observation from Tables 1 and 2 is that increasing Ω or decreasing Re^2/Ta causes, for a given F, a decrease in the annulus height.

Figure 2 shows examples for the obtained temperature profiles under both thermal conditions (I) and (0). It is clear from this figure that, for both boundary conditions, the temperature of the fluid increases as the flow moves away from

Table 1 F–L relationships for various values for a fluid of Pr = 0.7 in an annulus of $N = 0.9$, case (I)

	Dimensionless annulus height, L									
	$Re^2/Ta = 10$							$Re^2/Ta = 1$		
F/Ω	0.00	0.45	0.9	≥ 1.8	-0.45	-0.90	≤ -1.80	0.00	≤ -0.45	≥ 0.45
0.095	4.31×10^{-2}	4.08×10^{-2}	3.65×10^{-2}	NI*	4.34×10^{-2}	4.17×10^{-2}	NI	3.42×10^{-2}	NI	NI
0.09	1.73×10^{-2}	1.64×10^{-2}	1.47×10^{-2}	NI	1.74×10^{-2}	1.67×10^{-2}	NI	1.38×10^{-2}	NI	NI
0.08	6.98×10^{-3}	6.64×10^{-3}	6.00×10^{-3}	NI	7.02×10^{-3}	6.77×10^{-3}	NI	5.65×10^{-3}	NI	NI
0.07	3.80×10^{-3}	3.62×10^{-3}	3.27×10^{-3}	NI	3.82×10^{-3}	3.69×10^{-3}	NI	3.06×10^{-3}	NI	NI
0.06	2.23×10^{-3}	2.12×10^{-3}	1.91×10^{-3}	NI	2.24×10^{-3}	2.16×10^{-3}	NI	1.77×10^{-3}	NI	NI
0.05	1.32×10^{-3}	1.25×10^{-3}	1.12×10^{-3}	NI	1.33×10^{-3}	1.28×10^{-3}	NI	1.04×10^{-3}	NI	NI
0.04	7.52×10^{-4}	7.13×10^{-4}	6.36×10^{-4}	NI	7.55×10^{-4}	7.21×10^{-4}	NI	6.08×10^{-4}	NI	NI
0.03	3.92×10^{-4}	3.74×10^{-4}	3.36×10^{-4}	NI	3.92×10^{-4}	3.72×10^{-4}	NI	3.36×10^{-4}	NI	NI
0.02	1.76×10^{-4}	1.70×10^{-4}	1.55×10^{-4}	NI	1.75×10^{-4}	1.64×10^{-4}	NI	1.62×10^{-4}	NI	NI
0.01	5.53×10^{-5}	5.38×10^{-5}	4.93×10^{-5}	NI	5.43×10^{-5}	5.04×10^{-5}	NI	5.41×10^{-5}	NI	NI
0.005	NI	NI	NI	NI	NI	NI	NI	NI	NI	NI
0.001	NI	NI	NI	NI	NI	NI	NI	NI	NI	NI

* NI: Numerical instability occurs before the flow reaches the annulus exit cross section because of the presence of flow reversals within the domain of solution.

Table 2 F–L relationships for various values for a fluid of Pr = 0.7 in an annulus of $N = 0.9$, case (0)

	Dimensionless annulus height, L									
	$Re^2/Ta = 10$							$Re^2/Ta = 1$		
F/Ω	0.00	0.45	0.9	≥ 1.8	-0.45	-0.90	-1.80	0.00	≥ 0.45	≤ -0.45
0.095	4.05×10^{-2}	3.83×10^{-2}	3.42×10^{-2}	NI*	4.08×10^{-2}	3.91×10^{-2}	NI	3.24×10^{-2}	NI	NI
0.090	1.62×10^{-2}	1.54×10^{-2}	1.38×10^{-2}	NI	1.63×10^{-2}	1.57×10^{-2}	NI	1.31×10^{-2}	NI	NI
0.080	6.53×10^{-3}	6.22×10^{-3}	5.62×10^{-3}	NI	6.57×10^{-3}	6.37×10^{-3}	NI	5.37×10^{-3}	NI	NI
0.070	3.55×10^{-3}	3.38×10^{-3}	3.05×10^{-3}	NI	3.57×10^{-3}	3.44×10^{-3}	NI	2.91×10^{-3}	NI	NI
0.060	2.08×10^{-3}	1.98×10^{-3}	1.76×10^{-3}	NI	2.10×10^{-3}	2.02×10^{-3}	NI	1.69×10^{-3}	NI	NI
0.050	1.23×10^{-3}	1.16×10^{-3}	1.04×10^{-3}	NI	1.23×10^{-3}	1.18×10^{-3}	NI	9.88×10^{-4}	NI	NI
0.040	6.97×10^{-4}	6.59×10^{-4}	5.84×10^{-4}	NI	7.00×10^{-4}	6.67×10^{-4}	NI	5.62×10^{-4}	NI	NI
0.030	3.64×10^{-4}	3.45×10^{-4}	3.07×10^{-4}	NI	3.64×10^{-4}	3.45×10^{-4}	NI	2.97×10^{-4}	NI	NI
0.020	1.61×10^{-5}	1.54×10^{-4}	1.40×10^{-4}	NI	1.61×10^{-4}	1.53×10^{-4}	NI	1.33×10^{-4}	NI	NI
0.010	5.00×10^{-5}	4.83×10^{-5}	4.48×10^{-5}	NI	4.97×10^{-5}	4.75×10^{-5}	NI	3.86×10^{-5}	NI	NI
0.005	NI	NI	NI	NI	NI	NI	NI	NI	NI	NI

* NI: Numerical instability occurs before the flow reaches the annulus top exit due to the presence of flow reversals within the domain of solution.

Table 3 Adiabatic wall temperature against dimensionless axial distance, $N = 0.9$, Pr = 0.7

		Case (I)			Case (0)		
F	Z/Ω	0.0	0.9	-0.9	0.0	0.9	-0.9
0.03	2.00×10^{-8}	0.0000	0.0000	0.0000	0.0000	0.0000	0.0000
	3.13×10^{-5}	0.0002	0.0002	0.0002	0.0003	0.0003	0.0003
	1.06×10^{-4}	0.0532	0.0538	0.0538	0.0601	0.0600	0.0600
	1.56×10^{-4}	0.1351	0.1364	0.1363	0.1478	0.1478	0.1480
	L	0.4967	0.4386	0.4821	0.4926	0.4224	0.4766
0.09	2.00×10^{-6}	0.0000	0.0000	0.0000	0.0000	0.0000	0.0000
	1.30×10^{-4}	0.0015	0.0015	0.0015	0.0019	0.0019	0.0019
	6.30×10^{-4}	0.2221	0.2236	0.2232	0.2385	0.2368	0.2375
	1.13×10^{-3}	0.4579	0.4613	0.4580	0.4811	0.4772	0.4808
	2.13×10^{-3}	0.7362	0.7392	0.7358	0.7589	0.7556	0.7591
	3.13×10^{-3}	0.8704	0.8720	0.8701	0.8870	0.8853	0.8872
	1.06×10^{-2}	0.9992	0.9992	0.9992	0.9995	0.9995	0.9995
	L	1.0000	1.0000	1.0000	1.0000	1.0000	1.0000

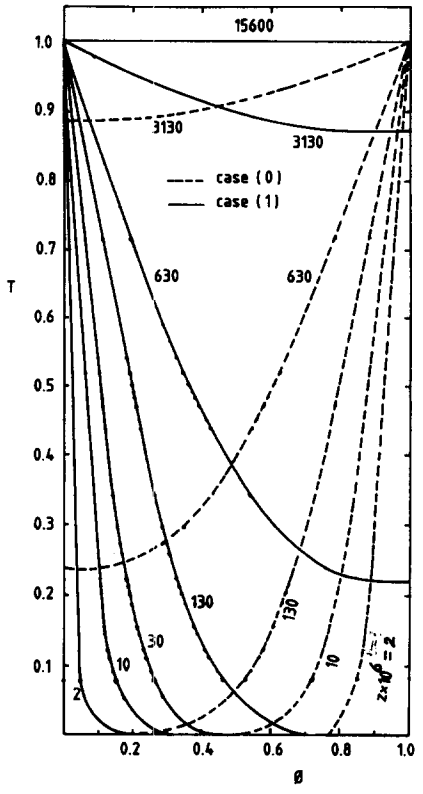

Figure 2 Temperature profiles: $N = 0.9$; Pr = 0.7; $\Omega = 0.45$; $F = 0.09$, $Re^2/Ta = 10$

the entrance cross section (i.e., value of Z increases). Also, because Figure 2 is for a relatively large value of F, the dimensionless temperature T approaches its fully developed value ($T = 1$) as the flow approaches the exit cross section. However, near the annulus entrance (small values of Z) the fluid temperature is affected only near the heated boundary.

Engineers are usually concerned with the mixing cup temperature T_m and the heat gained or lost H by the fluid, rather than the details of the temperature field. Figure 3 gives

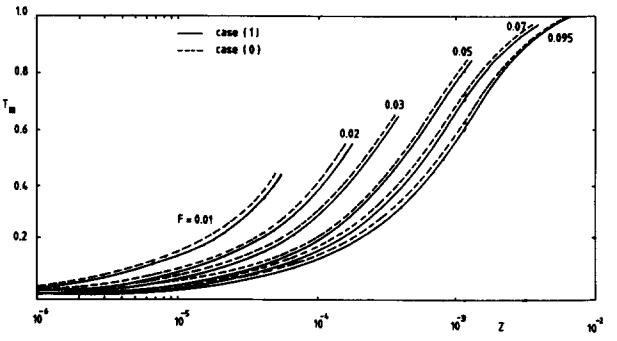

Figure 3 Mixing cup temperature against axial distance: $N = 0.9$; Pr = 0.7; $\Omega = 0$; $Re^2/Ta = 10$

the variation of the mixing cup temperature T_m with the dimensionless axial distance Z for both thermal boundary conditions (I) and (0) in an annulus of $N = 0.9$ with Ω. This figure can be used for other values of Ω, as long as the flow remains laminar, because it has been found, from the obtained results, that the outer cylinder rotation has very slight and negligible effect on the temperature field. To clarify this point and to give other thermal parameters of importance to engineers, Tables 3 and 4 give the dimensionless heat absorbed H and the adiabatic wall temperature T_{ad} against the dimensionless axial distance Z for a relatively large value of F (0.09), a relatively small value of F (0.01), and thermal conditions (I) and (0). In thse two tables, values of H and T_{ad} are given at three chosen values of Ω; namely, $\Omega = 0.0$, 0.9, and -0.9. It is clear from the results presented in these two tables that the outer cylinder rotation has only a negligible effect on the heat absorbed and the adiabatic wall temperature over the investigated range of Ω.

Acknowledgments

The authors are indebted to S. Kewan for running the program on the VAX computer of the Jordan University of Science and Technology.

Table 4 Dimensionless heat absorbed against dimensionless axial distance, $N = 0$. Pr = 0.7

		Case (1)			Case (0)		
F	Z/Ω	0.0	0.9	−0.9	0.0	0.9	−0.9
0.03	2.00×10^{-8}	0.00000	0.00000	0.00000	0.00049	0.00049	0.00049
	1.00×10^{-7}	0.00002	0.00002	0.00002	0.00050	0.00050	0.00050
	3.00×10^{-7}	0.00010	0.00010	0.00010	0.00053	0.00053	0.00052
	1.30×10^{-6}	0.00035	0.00035	0.00035	0.00064	0.00063	0.00063
	6.30×10^{-6}	0.00086	0.00086	0.00086	0.00106	0.00106	0.00106
	3.13×10^{-5}	0.00217	0.00217	0.00217	0.00240	0.00238	0.00238
	1.56×10^{-4}	0.00581	0.00585	0.00582	0.00617	0.00613	0.00616
	L	0.00970	0.00912	0.00955	0.00979	0.00905	0.00962
0.09	2.00×10^{-6}	0.00057	0.00058	0.00058	0.00165	0.00164	0.00164
	1.00×10^{-5}	0.00178	0.00179	0.00179	0.00242	0.00240	0.00240
	3.00×10^{-5}	0.00328	0.00329	0.00329	0.00385	0.00385	0.00381
	1.30×10^{-4}	0.00764	0.00767	0.00767	0.00834	0.00827	0.00827
	6.30×10^{-4}	0.01986	0.02000	0.01987	0.02092	0.02075	0.02089
	3.13×10^{-3}	0.04087	0.04093	0.04087	0.04150	0.04145	0.04145
	L	0.04511	0.04511	0.04511	0.04511	0.04511	0.04511

References

Astill, K. N. 1964. Studies of the developing flow between concentric cylinders with the inner cylinder rotating. *J. Heat Transfer*, **86**, 383–392

Aung, W. 1972. Fully developed laminar free convection between vertical plates heated asymmetrically. *Int. J. Heat Mass Transfer*, **15**, 1577–1580

Becker, K. M. and Kaye, J. 1962. The influence of a radial temperature gradient on the instability of fluid flow in an annulus with an inner rotating cylinder. *J. Heat Transfer*, **84**, 106–110

Chung, K. C. and Astill, K. N. 1977. Hydrodynamic instability of viscous flow, between rotating coaxial cylinders with fully developed axial flow. *J. Fluid Mech.*, **81**, 641–655

Coney, J. E. R. and El-Shaarawi, M. A. I. 1974a. A contribution to the numerical solution of developing laminar flow in the entrance region of concentric annuli with rotating inner walls. *J. Fluids Eng.* **96**, 333–340

Coney, J. E. R. and El-Shaarawi, M. A. I. 1974b. Laminar heat transfer in the entrance region of concentric annuli with rotating inner walls. *J. Heat Transfer*, **96**, 560–562

El-Shaarawi, M. A. I., and Sarhan, A. 1981. Developing laminar free convection in an open ended vertical annulus with a rotating inner cylinder. *J. Heat Transfer*, **103**, 553–558

El-Shaarawi, M. A. I. and Khamis, M. 1987. Induced flow in uniform heated vertical annuli with rotating inner walls, *Num. Heat Transfer*, **12**, 493–508

El-Shaarawi, M. A. I. and Kodah, Z. 1990. Natural convection in an annulus with two rotating boundaries. *JSME Int. J.*, **33**, 316–325

Schlichting, H. 1979. Boundary layer theory. McGraw Hill, New York

Simmers, D. A. and Coney, J. E. R. 1980. Velocity distributions in Taylor vortex flow with imposed laminar axial flow and isothermal surface heat transfer. *Int. J. Heat Fluid Flow*, **2**, 85–91

Soundalgeker, V. M. and Sarma, P. R. L. 1986. Finite-difference solution of laminar developing flow in an annulus between two rotating cylinders. *Appl. Energy*, 47–60

Taylor, G. I. 1923. Stability of a viscous liquid contained between two rotating cylinders. *Phil. Trans.*, **223**, 289–343

Walowit, J., Tsao, S. and Diprima, R. C. 1964. Stability of flow between arbitrarily spaced concentric surfaces including the effect of a radial temperature gradient. *J. Applied Mech.*, **31**, 585–593

Wan, C. C. and Coney, J. E. R. 1982. An investigation of adiabatic spiral vortex flow in wide gaps by visualization and digital analysis. *Int. J. Heat Fluid Flow*, **3**, 39–44